UvA-DARE (Digital Academic Repository)

Excited-State Decay Pathways of Molecular Rotors: Twisted Intermediate or Conical Intersection?

Suhina, T.; Amirjalayer, S.; Mennucci, B.; Woutersen, S.; Hilbers, M.; Bonn, D.; Brouwer, A.M.

Link to publication

Excited-State Decay Pathways of Molecular Rotors: Twisted Intermediate or Conical Intersection?

Tomislav Suhina,[†,‡] Saeed Amirjalayer,[§] Benedetta Mennucci,[∥] Sander Woutersen,[*,†] Michiel Hilbers,[†] Daniel Bonn,[‡] and Albert M. Brouwer[*,†]

[†]van 't Hoff Institute for Molecular Sciences, University of Amsterdam, P.O. Box 94157, 1090 GD Amsterdam, The Netherlands

[‡]van der Waals-Zeeman Institute, Institute of Physics, University of Amsterdam, P.O. Box 94485, 1090 GL Amsterdam, The Netherlands

[§]Center for Nanotechnology (CeNTech) and Physical Institute, University of Münster, Heisenbergstrasse 11, 48149 Münster, Germany

[∥]Dipartimento di Chimica e Chimica Industriale, University of Pisa, via G. Moruzzi 13, 56124 Pisa, Italy

S *Supporting Information*

ABSTRACT: The fluorescence intensity of molecular rotors containing the dicyanomethylenedihydrofuran (DCDHF) motif increases strongly with solvent viscosity. Single-bond and double-bond rotations have been proposed as pathways of nonradiative decay for this and related molecular rotors. We show here that both are involved in the case of DCDHF rotors: Fluorescence is quenched by rotation around the dicyanomethylene double bond in nonpolar solvents, but in a sufficiently polar environment rotation about a formally single bond leads to a dark internal charge-transfer state.
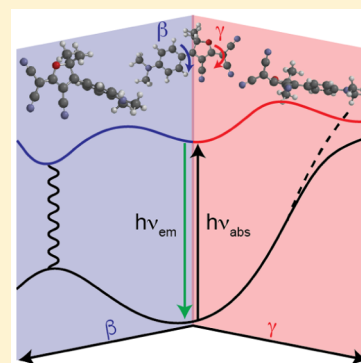
Molecular rotors with a viscosity-dependent fluorescence deactivation pathway are widely used as molecular viscosity probes in biology,[1−6] fluid dynamics,[7−9] and materials science.[10−15] We have recently shown that such molecules (**1** and **2** in Scheme 1) comprise a unique tool in studying contact mechanics, enabling us for the first time to directly visualize contacts between solid surfaces on a molecular scale.[16]

The photophysics of these remarkably useful probes and functionally similar malononitriles are still incompletely understood and actively debated.[10,13,15,17−24] In a model proposed by Willets,[21] fluorescence deactivation of **1** occurs through an irreversible twist involving the dicyanomethylene bond (γ in Scheme 1), upon which the ground- and the excited-state potential energy surfaces (PESs) come into sufficiently close proximity to allow efficient deactivation. We have recently reported nonexponential fluorescence decays for **1** in some solvents,[16] indicating that its photophysical behavior is complex. Interestingly, in the case of 9-(2,2-dicyanovinyl)-julolidine (DCVJ, see Scheme 1), nonexponential fluorescence decays have also been observed. To explain this observation, Dreger proposed a model involving a dark twisted state that equilibrates with a planar locally excited (LE) state.[14] In a more recent study, Gaffney and coworkers[19] studied time-resolved infrared anisotropy of DCVJ in DMSO and showed that the LE state decays to a hot ground state and to a twisted intermediate species in DMSO. This branching may be different in other

Scheme 1. Molecular Structures of 9-(2,2-Dicyanovinyl)julolidine and the Dicyanomethylenedihydrofuran Derivatives 1 and 2 Investigated Here[a]
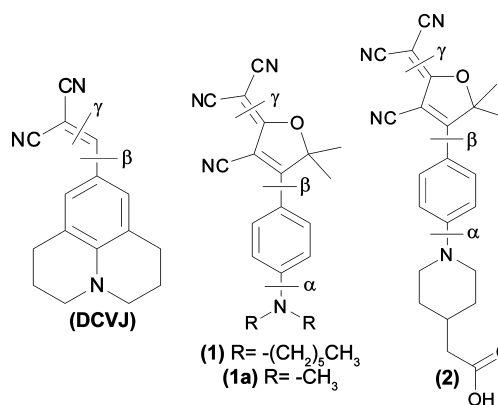
[a]**1a** is simplified analogue of **1** that was used in TD-DFT calculations.

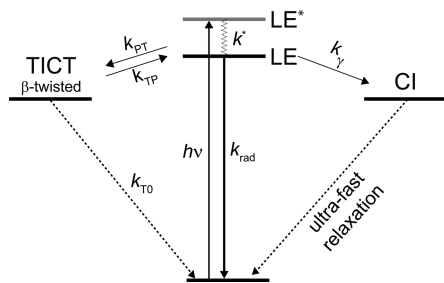solvents and may in turn present a cause for observed variations in the viscosity response.[18]

The two proposed fluorescence deactivation pathways of **1** and **2** are presented in Scheme 2. After initial photoexcitation

Scheme 2. Proposed Model for Fluorescence Deactivation of 1

from the ground-state (GS) and fast relaxation processes (with rate constant $k*$), the molecule reaches the near-planar LE state. From there it can radiatively relax to the ground state (k_{rad}) or perform twisting motion around either the γ (k_γ)[21] or β (k_{PT}) bond (see Scheme 1). Both twists result in fluorescence deactivation. Twisting around γ leads to a conical intersection (CI) with the ground-state PES and instantaneous nonradiative relaxation. Twisting around the β bond yields a highly polar TICT[25] state. This state has a finite lifetime, and it can either act as a sink (it converts to the GS directly with rate constant k_{T0}) or as a reservoir state (TICT back-converts to the LE state and to the GS with rate constants k_{TP} and k_{T0}, respectively). In the latter case delayed fluorescence occurs and causes biexponential fluorescence decays. These twists occur easily in liquid solvents but become hindered as solvent viscosity increases. In this way, the degree of confinement is reflected by a fluorescence response. Below we show that the deactivation pathway of **1** strongly depends on solvent polarity: Deactivation proceeds through CI (through γ twist in Scheme 1) in nonpolar solvents, whereas polar solvents facilitate the formation of the TICT species and subsequent deactivation (through β twist, Scheme 1).

In this work, we use steady-state and time-resolved fluorescence measurements and combine them with visible pump mid-IR probe transient measurements. Combination of these powerful techniques enables us to learn more about the

excited-state dynamics of **1** in a range of solvents. To further deepen our fundamental understanding of the relevant processes, we supplement our experimental findings with TD-DFT calculations.

The steady-state absorption and fluorescence spectra of **1** (see Figure 1a) show significant changes in both the shape and peak positions as solvents are changed from nonpolar hexane to the highly polar DMSO, indicating charge-transfer character of the excited state. From the Stokes shifts we estimate the difference in dipole moments of S_1 and S_0 to be $\Delta\mu = 5.8 \pm 0.9$ D.[22,23,26] Because of efficient fluorescence deactivation, quantum yields in liquids are very low (see Figure 1a inset and Table 1). In the very polar solvents DMSO and MeCN the

Table 1. Fluorescence Properties of 1 at Room Temperature (24 °C)

solvent	η/cP[a]	ϵ_r[a]	Φ_f/%[b]	$k_{rad} \times 10^8$/s^{-1}[d]
hexane	0.30	1.9	~0.6	2.8
toluene	0.56	2.4	5.0	3.1
EtOAc	0.42	6.0	2.9[c]	2.8
MeCN	0.37	36.6	~0.3	2.8
DMSO	1.99	46.8	~0.5	3.0

[a]Values for relative permittivity (ϵ_r) and viscosity (η) obtained from ref 27. [b]For fluorescence quantum yields fluorescein in 0.1 M NaOH ($\Phi_f = 0.89$[28]) was used as a reference. [c]Φ_f obtained from ref 16. [d]Radiative rates from the Strickler–Berg expression.

quantum yields (Φ_f) are <1%. This value is somewhat higher in medium polarity EtOAc (2.9%) and peaks in the relatively nonpolar toluene (5.0%). An order-of-magnitude drop in Φ_f (~0.6%) is observed when going from toluene to the even less polar hexane (Figure 1a, inset). This trend can be explained by the presence of two different barriers with different polarity dependencies that lead to fluorescence deactivation.

The fluorescence decays show trends similar to the ones observed in steady-state measurements. In hexane, the decays are too fast to be measured with our TCSPC equipment. In toluene, fluorescence decay is monoexponential and relatively slow (120 ps). Our calculations (see below) indicate that the increase in polarity (which occurs in the case of hexane vs toluene) results in an increase in the energy barrier that separates the LE state from the CI. In EtOAc, the decay is biexponential (with time constants of $\tau_1 = 30$ and $\tau_2 = 228$ ps at

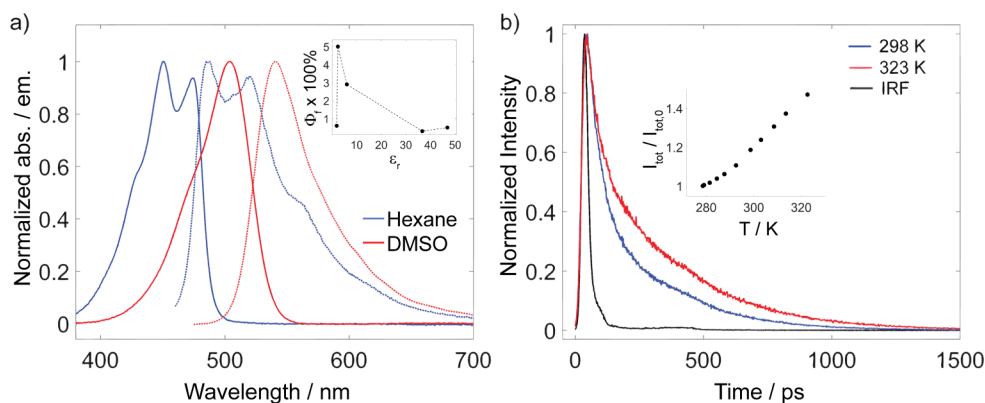**Figure 1.** (a) Steady-state absorption (solid lines) and fluorescence (dotted lines) spectra of **1** in hexane and DMSO. Inset: Φ_f (in hexane, toluene, EtOAc, MeCN, and DMSO) versus relative permittivity. (b) Time-correlated single photon counting traces of **1** in EtOAc measured at different temperatures. Inset: Integrated fluorescence intensity (normalized by the total intensity measured at 5.4 °C) versus temperature.
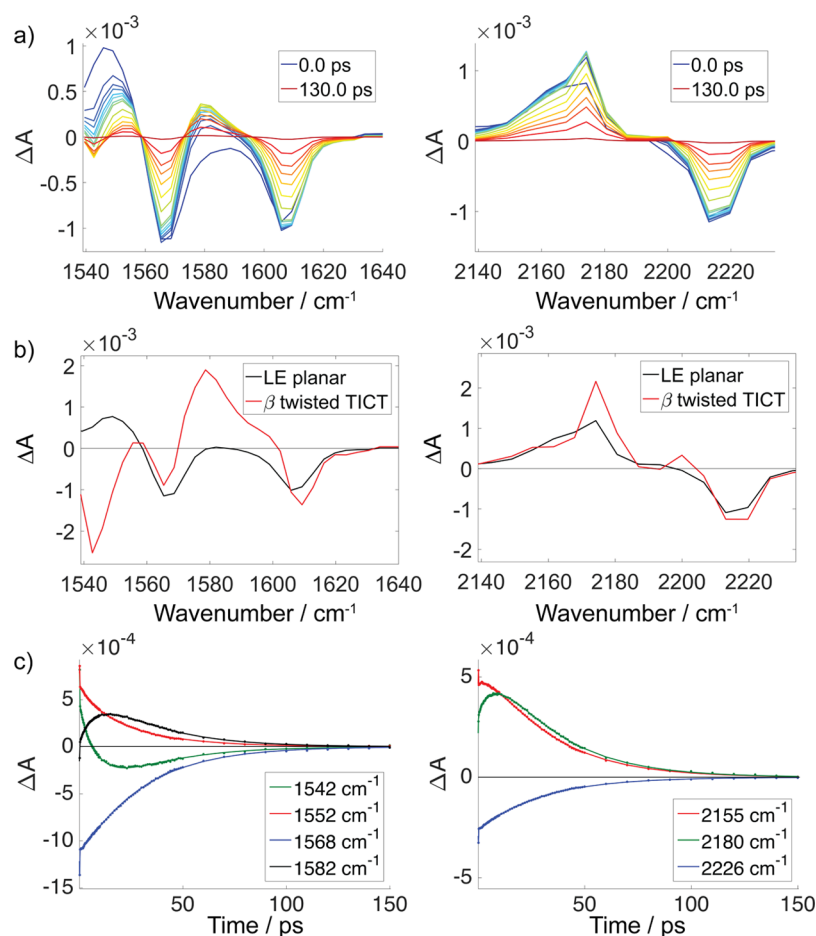
Figure 2. Time-resolved infrared spectra of **1** in DMSO measured by vis-pump (λ_{exc} = 488 nm) mid-IR probe spectroscopy. (a) Spectral traces measured in C=C (left) and CN (right) stretch regions. (b) Reconstructed species associated spectra for C=C (left) and CN (right) regions. (c) Representative time traces and fits obtained for C=C (left) and CN (right) regions.

room temperature, Figure 1b). Reconstructed decay-associated fluorescence spectra show two components with identical spectral profiles (Figure S14), indicating that fluorescence emission occurs from a single state. The trend obtained from calculations presented below suggests that EtOAc is just polar enough to prevent crossing at the energy barrier leading to the CI (the γ twist becomes hindered) and to simultaneously lower the energy barrier that separates the LE state from the β-twisted (TICT) state. It is, however, not polar enough to stabilize the TICT state to such an extent that it cannot convert back to the fluorescent planar LE state. As a result of this interconversion we observe delayed fluorescence. The kinetic model (see Scheme 2) can be expressed by the following equations

$$\frac{d[P]}{dt} = k_{TP}[T] - k_{PT}[P] - k_{rad}[P] \tag{1}$$

$$\frac{d[T]}{dt} = k_{PT}[P] - k_{TP}[T] - k_{T0}[T] \tag{2}$$

$$[GS] = 1 - [P] - [T] \tag{3}$$

(where P, T, and GS are the planar, TICT, and ground state, respectively), which can be solved analytically, so that k_{PT}, k_{TP}, and k_{T0} can be obtained from our data. The k_{PT} and k_{TP} values thus obtained allow estimation of the energy of the TICT state to be ~0.9 kcal/mol lower than the energy of the planar LE state at room temperature for **1** in EtOAc.

Fluorescence emission spectra measured at increasing temperatures show an unusual increase in intensities with temperature (Figure 1b, inset). To further investigate this, we have measured fluorescence decays for **1** in EtOAc at different temperatures (see Figure 1b and Table S2). The twisting rates k_{PT} and k_{TP} increase with temperature, while k_{T0} somewhat counterintuitively decreases. This causes the shorter time constant (τ_1) to decrease (from 37 ps at 5.5 °C to 25 ps at 54.5 °C) and the longer one (τ_2) to increase (from 168 ps at 5.5 °C to 282 ps at 54.5 °C). Two factors contribute to the increase in Φ_f with increasing temperature: (1) Nonradiative relaxation of **1** in EtOAc occurs through the TICT state; the decrease in k_{T0} results in less efficient nonradiative decay. (2) The simultaneous increase in k_{TP}/k_{PT} produces an increase in population of the fluorescent planar state (P). The change in k_{T0} probably originates from the fact that increasing the temperature causes the relative permittivity of EtOAc to decrease from ~6.4 (5.5 °C) to ~5.4 (54 °C),[27] which, in turn, destabilizes the TICT state and separates it further from the GS PES rendering nonradiative decay less rapid.[29] At the same time, the energy of the TICT state comes closer to the energy of the LE state, increasing k_{TP}. The increase in Φ_f and longer τ_2 with temperature (Figure 1b) show that the escape through the alternative channel (γ twist) does not occur under these conditions.

In DMSO, the TICT state (β-twisted structure in Scheme 2) readily forms and does not revert back to the fluorescent LE
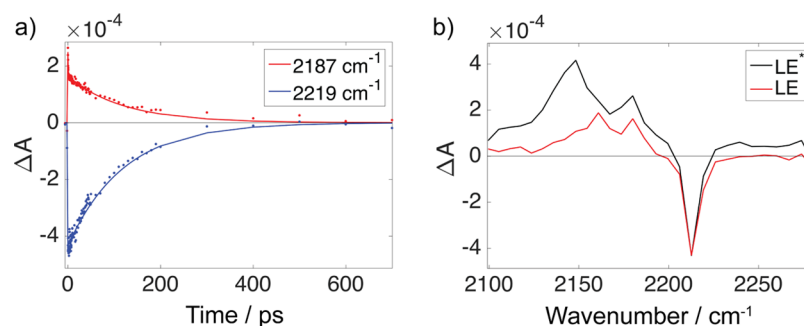
Figure 3. (a) Representative time traces of **1** in toluene. (b) Species-associated spectra obtained from global analysis with sequential model assumed.

planar state. The formation of the β-twisted transient species in polar DMSO can be observed in vis-pump mid-IR probe measurements (time resolution ~200 fs). Transient IR spectral traces for **1** in DMSO measured in the C≡C and CN regions are shown in Figure 2a. Representative time traces are shown in Figure 2c. In the C≡C region, ground-state bleach (GSB) bands are centered at 1568 and 1608 cm^{-1}. Another GSB band is centered at 1542 cm^{-1}, but its strong overlap with excited-state absorption (ESA) bands originating from the planar LE state makes it visible only at later probe delays. An excited-state band rises at 1582 cm^{-1}, and we attribute it to the formation of the β-twisted TICT state. Its rise correlates with the decay of LE ESA bands centered at 1535 and 1552 cm^{-1} (Figure 2a,c, left side), indicating sequential formation kinetics. A spectral signature of this species can also be observed in the CN stretch region (see Figure 2a,c, right side). The TICT state manifests itself here as a rise in the ESA, but very pronounced overlap between the CN bands (symmetric and asymmetric stretches) of the LE and TICT states complicates the separation of the bands associated with the two species. From a global fit of the transient data with a target sequential model[30] (see eq 4 and the Supporting Information for details), we reconstruct species-associated spectra (shown in Figure 2b), with rate constants of $k_{PT} = (3.68 \pm 0.06) \times 10^{-2}$ ps^{-1} and $k_{T0} = (9.85 \pm 0.03) \times 10^{-2}$ ps^{-1} (k^* was too fast to be resolved).

$$S_{1,LE^*} \xrightarrow{k^*} S_{1,LE} \xrightarrow{k_{PT}} S_{1,\beta(TICT)} \xrightarrow{k_{T0}} S_0 \qquad (4)$$
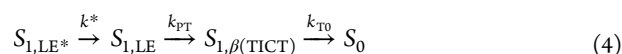
Vis-pump mid-IR probe measurements for **1** in toluene do not indicate the presence of transient species. Global analysis with sequential model yields two rate constants of 1.31 ± 0.07 and $(8.32 \pm 0.02) \times 10^{-3}$ ps^{-1} (Figure 3). We attribute the shorter one to vibrational cooling and the longer one to the decay of the fluorescent LE state. These rates show excellent agreement with the fluorescence measurements and indicate that fluorescence deactivation of **1** indeed proceeds through CI and does not involve transient intermediates.

Relaxed scans of the excited-state PES for **1a** obtained by TD-DFT (CAM-B3LYP/6-31+G(d)) calculations, where solvent effects are included using the polarizable continuum model (PCM),[31] show excellent agreement with our experimental results. TD-DFT calculations find three minima (see Figure 4 and Scheme 2) on the S$_1$ PES. One minimum belongs to the fluorescent LE planar state, which is reached upon photoexcitation and subsequent relaxation. A second minimum is reached by twisting about the γ bond (see Scheme 2). The sudden drop in oscillator strength and the close proximity of the GS and ES PES (see Figure 4a and inset) both suggest the presence of a CI near these coordinates. This is in excellent agreement with the initially proposed deactivation model[21] and
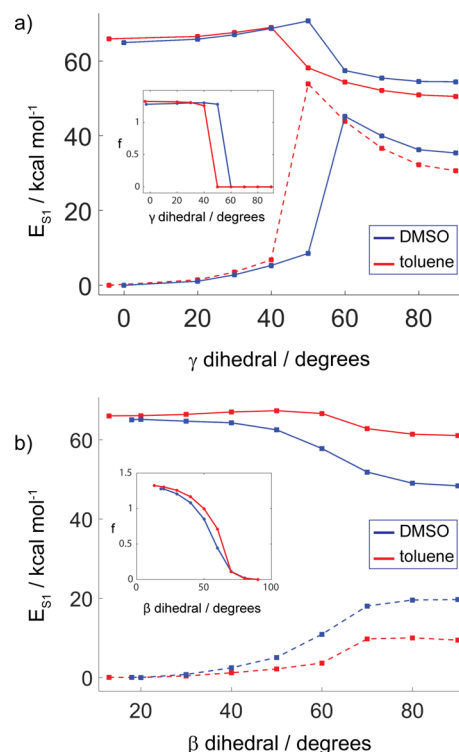

Figure 4. Potential energy surface scans of **1a** with polarizable continuum model solvation. Insets show oscillator strength as a function of scanned dihedral angle. Ground-state energies are calculated at excited-state geometries. (a) Relaxed γ-constrained scan. (b) Relaxed β-constrained scan.

identifies this twist as an important fluorescence deactivation pathway. Our calculations indicate that the dipole moment decreases as the twist advances, which, in turn, results in polar solvents hindering this twist. Such a trend was observed previously by Massin et al., who used deactivation through a dicyanomethylene twist to probe medium polarity.[32] Consequently, this pathway is expected to be less favorable in polar solvents (calculated barriers are 3.1 and 5.8 kcal/mol for toluene and DMSO, respectively). We have experimentally estimated (see Supporting Information) this barrier to be ~3.6 kcal mol^{-1} in hexane ($\epsilon_r = 1.89$) and toluene ($\epsilon_r = 2.38$). This value is reasonably close to the calculated value of 3.1 kcal mol^{-1} obtained for toluene. The third PES minimum can be accessed through twisting of the β bond (Scheme 2 and Figure 4b). It is accompanied by a large increase in the calculated dipole moment and a gradual drop in the oscillator strength. A polar environment stabilizes this highly polar state and lowers the energy barrier that separates it from the LE planar state

(from 1.3 kcal mol^{-1} in toluene to 0.1 kcal mol^{-1} in DMSO). This makes the β-twisted TICT state easier to reach but hinders the back conversion from the TICT to the planar fluorescent state when the environment is too polar. The energy difference between the GS and ES twisted geometries decreases as polarity increases (from 52 kcal mol^{-1} in toluene to 29 kcal mol^{-1} in DMSO), but the surfaces still remain well-separated and the oscillator strengths decrease gradually with increasing β. We have found no evidence of a CI near these coordinates. Instead, nonradiative relaxation from this state is expected (and experimentally observed) to become more efficient as the solvent polarity increases due to the increasing proximity of the two surfaces (energy-gap law).[29] The trends obtained from the TD-DFT calculations are in excellent agreement with our experimental observations that show that reversible β twist occurs in solvents of medium polarity (EtOAc) and becomes irreversible as polarity increases further (DMSO, MeCN) due to stabilization of the TICT state.

To conclude, we have shown that **1** (and by analogy, **2**) can relax to the ground state via two distinct pathways. Both involve significant changes in geometry and account for the sensitivity of the fluorescence of these molecules to viscosity and free volume. The relaxation pathway depends strongly on the dielectric properties of the molecular environment: In nonpolar solvents relaxation occurs by twisting about the exocyclic C=C (γ) bond, which results in momentary deactivation. Polar solvents hinder this twist, while at the same time opening up a new deactivation pathway that leads to the dark intermediate β twisted ICT state from which the nonradiative relaxation occurs. The presence of two decay pathways leads to a discontinuous dependence of the nonradiative decay rate at low viscosities on the polarity. Because the two pathways have different spatial requirements, the dependences of their rates on viscosity and free volume may be different. These factors need to be taken into account when molecular rotors similar to **1** are used as viscosity/free volume sensors.

ASSOCIATED CONTENT

Ⓢ Supporting Information

The Supporting Information is available free of charge on the ACS Publications website at DOI: 10.1021/acs.jpclett.6b02277.

> Steady-state experiments, temperature and time-resolved measurements; computational details; kinetic modeling of time-resolved data. (PDF)

AUTHOR INFORMATION

Corresponding Authors
*S.W.: E-mail: s.woutersen@uva.nl;
*A.M.B.: E-mail: a.m.brouwer@uva.nl.

Notes

The authors declare no competing financial interest.

ACKNOWLEDGMENTS

REFERENCES

(1) Biancalana, M.; Koide, S. Molecular mechanism of Thioflavin-T binding to amyloid fibrils. *Biochim. Biophys. Acta, Proteins Proteomics* **2010**, *1804*, 1405−1412.

(2) Willets, K. A.; Ostroverkhova, O.; He, M.; Twieg, R. J.; Moerner, W. Novel fluorophores for single-molecule imaging. *J. Am. Chem. Soc.* **2003**, *125*, 1174−1175.

(3) Lord, S. J.; Conley, N. R.; Lee, H.-l. D.; Samuel, R.; Liu, N.; Twieg, R. J.; Moerner, W. A photoactivatable push- pull fluorophore for single-molecule imaging in live cells. *J. Am. Chem. Soc.* **2008**, *130*, 9204−9205.

(4) Lord, S. J.; Lu, Z.; Wang, H.; Willets, K. A.; Schuck, P. J.; Lee, H.-l. D.; Nishimura, S. Y.; Twieg, R. J.; Moerner, W. Photophysical properties of acene DCDHF fluorophores: Long-wavelength single-molecule emitters designed for cellular imaging. *J. Phys. Chem. A* **2007**, *111*, 8934−8941.

(5) López-Duarte, I.; Vu, T. T.; Izquierdo, M. A.; Bull, J. A.; Kuimova, M. K. A molecular rotor for measuring viscosity in plasma membranes of live cells. *Chem. Commun.* **2014**, *50*, 5282−5284.

(6) Dent, M. R.; López-Duarte, I.; Dickson, C. J.; Geoghegan, N. D.; Cooper, J. M.; Gould, I. R.; Krams, R.; Bull, J. A.; Brooks, N. J.; Kuimova, M. K. Imaging phase separation in model lipid membranes through the use of BODIPY based molecular rotors. *Phys. Chem. Chem. Phys.* **2015**, *17*, 18393−18402.

(7) Rumble, C.; Rich, K.; He, G.; Maroncelli, M. CCVJ is not a simple rotor probe. *J. Phys. Chem. A* **2012**, *116*, 10786−10792.

(8) Mustafic, A.; Huang, H.-M.; Theodorakis, E. A.; Haidekker, M. A. Imaging of flow patterns with fluorescent molecular rotors. *J. Fluoresc.* **2010**, *20*, 1087−1098.

(9) Mustafic, A.; Elbel, K. M.; Theodorakis, E. A.; Haidekker, M. Apparent Shear Sensitivity of Molecular Rotors in Various Solvents. *J. Fluoresc.* **2015**, *25*, 729−738.

(10) Loutfy, R. O. High-conversion polymerization of fluorescence probes. 1. Polymerization of methyl methacrylate. *Macromolecules* **1981**, *14*, 270−275.

(11) Royal, J. S.; Torkelson, J. M. Monitoring the molecular scale effects of physical aging in polymer glasses with fluorescence probes. *Macromolecules* **1990**, *23*, 3536−3538.

(12) Royal, J. S.; Torkelson, J. M. Molecular-scale asymmetry and memory behavior in poly (vinyl acetate) monitored with mobility-sensitive fluorescent molecules. *Macromolecules* **1992**, *25*, 1705−1710.

(13) Dreger, Z.; Lang, J.; Drickamer, H. High pressure study of flexible fluorescent dye molecules in solid polymeric media. I. Julolidinemalononitrile. *Chem. Phys.* **1993**, *169*, 351−359.

(14) Dreger, Z.; White, J.; Drickamer, H. High pressure-controlled intramolecular-twist of flexible molecules in solid polymers. *Chem. Phys. Lett.* **1998**, *290*, 399−404.

(15) Jee, A.-Y.; Bae, E.; Lee, M. Internal twisting dynamics of dicyanovinyljulolidine in polymers. *J. Phys. Chem. B* **2009**, *113*, 16508−16512.

(16) Suhina, T.; Weber, B.; Carpentier, C. E.; Lorincz, K.; Schall, P.; Bonn, D.; Brouwer, A. M. Fluorescence Microscopy Visualization of Contacts Between Objects. *Angew. Chem., Int. Ed.* **2015**, *54*, 3688−3691.

(17) Abdel-Mottaleb, M.; Loutfy, R. O.; Lapouyade, R. Non-radiative deactivation channels of molecular rotors. *J. Photochem. Photobiol., A* **1989**, *48*, 87−93.

(18) Howell, S.; Dakanali, M.; Theodorakis, E. A.; Haidekker, M. A. Intrinsic and extrinsic temperature-dependency of viscosity-sensitive fluorescent molecular rotors. *J. Fluoresc.* **2012**, *22*, 457−465.

(19) Zhang, W.; Lan, Z.; Sun, Z.; Gaffney, K. J. Resolving photo-induced twisted intramolecular charge transfer with vibrational anisotropy and TDDFT. *J. Phys. Chem. B* **2012**, *116*, 11527−11536.

(20) Mqadmi, S.; Pollet, A. Non-radiative deactivation of p-(N, N-dialkylamino) benzylidenemalononitriles. *J. Photochem. Photobiol., A* **1990**, *53*, 275−281.

(21) Willets, K. A.; Callis, P. R.; Moerner, W. Experimental and theoretical investigations of environmentally sensitive single-molecule fluorophores. *J. Phys. Chem. B* **2004**, *108*, 10465−10473.

(22) Jin, H.; Liang, M.; Arzhantsev, S.; Li, X.; Maroncelli, M. Photophysical characterization of benzylidene malononitriles as probes of solvent friction. *J. Phys. Chem. B* **2010**, *114*, 7565−7578.

(23) Dahl, K.; Biswas, R.; Ito, N.; Maroncelli, M. Solvent dependence of the spectra and kinetics of excited-state charge transfer in three (alkylamino) benzonitriles. *J. Phys. Chem. B* **2005**, *109*, 1563−1585.

(24) Haidekker, M.; Brady, T.; Lichlyter, D.; Theodorakis, E. Effects of solvent polarity and solvent viscosity on the fluorescent properties of molecular rotors and related probes. *Bioorg. Chem.* **2005**, *33*, 415−425.

(25) Grabowski, Z. R.; Rotkiewicz, K.; Rettig, W. Structural changes accompanying intramolecular electron transfer: focus on twisted intramolecular charge-transfer states and structures. *Chem. Rev.* **2003**, *103*, 3899−4032.

(26) Mataga, N.; Kaifu, Y.; Koizumi, M. Solvent effects upon fluorescence spectra and the dipolemoments of excited molecules. *Bull. Chem. Soc. Jpn.* **1956**, *29*, 465−470.

(27) Haynes, W. M. *CRC Handbook of Chemistry and Physics*: CRC Press, 2014.

(28) Würth, C.; Grabolle, M.; Pauli, J.; Spieles, M.; Resch-Genger, U. Relative and absolute determination of fluorescence quantum yields of transparent samples. *Nat. Protoc.* **2013**, *8*, 1535−1550.

(29) Englman, R.; Jortner, J. The energy gap law for radiationless transitions in large molecules. *Mol. Phys.* **1970**, *18*, 145−164.

(30) van Stokkum, I. H. M.; Larsen, D. S.; van Grondelle, R. Global and target analysis of time-resolved spectra. *Biochim. Biophys. Acta, Bioenerg.* **2004**, *1657*, 82−104.

(31) Tomasi, J.; Mennucci, B.; Cammi, R. Quantum mechanical continuum solvation models. *Chem. Rev.* **2005**, *105*, 2999−3093.

(32) Massin, J.; Charaf-Eddin, A.; Appaix, F.; Bretonniere, Y.; Jacquemin, D.; Van Der Sanden, B.; Monnereau, C.; Andraud, C. A water soluble probe with near infrared two-photon absorption and polarity-induced fluorescence for cerebral vascular imaging. *Chem. Sci.* **2013**, *4*, 2833−2843.